Hydroxy double salts intercalated with Mn(II) complexes as potential T_1 contrast agents

Miao Jin,[a] Wanjing Li,[a] Dominic E. M. Spillane,[b] Carlos F. G. C. Geraldes,[c] Gareth R. Williams,[a]* and S. W. Annie Bligh[d]*

a. UCL School of Pharmacy, University College London, 29-39 Brunswick Square, London, WC1N 1AX, UK.

b. School of Human Sciences, London Metropolitan University, 166-220 Holloway Road, London, N7 8DB, UK.

c. Department of Life Sciences and Coimbra Chemistry Center - CQC, Faculty of Science and Technology, University of Coimbra, Coimbra, Portugal

d. Faculty of Science and Technology, University of Westminster, 115 New Cavendish Street, London, W1W 6UW, UK.

* Authors for correspondence. Tel: +44 (0) 207 753 5868 (GRW); +44 (0) 207 911 5038 (SWAB). Email: g.williams@ucl.ac.uk (GRW); a.bligh@westminster.ac.uk (SWAB).

Abstract

A series of Mn(II) aminophosphonate complexes were successfully synthesized and intercalated into the hydroxy double salt $[Zn_5(OH)_8]Cl_2{\cdot}yH_2O$. Complex incorporation led to an increase in the interlayer spacing from 7.8 to 10 – 12 Å. Infrared spectroscopy showed the presence of the characteristic vibration peaks of the Mn(II) complexes in the intercalates' spectra, indicating successful incorporation. The complex-loaded composites had somewhat lower proton relaxivities than the pure complexes. Nevertheless, these intercalates may have use as MRI contrast agents for patients with poor kidney function, where traditional Gd(III)-based contrast agents cause severe renal failure.

Keywords

Hydroxy double salt; magnetic resonance imaging; contrast agent; Mn complexes

1. Introduction

Magnetic resonance imaging (MRI) is a powerful technique for the investigation of soft tissue abnormalities. It has excellent spatial resolution, can be applied non-invasively, and does not require potentially harmful ionizing radiation. However, to obtain images of sufficient quality to permit a diagnosis to be made, a contrast agent is needed to permit discrimination between different tissue types. To date, Gd-based contrast agents have been effectively used to enhance the longitudinal (r_1) and transverse (r_2) relaxation times of water protons, thus improving the clarity of images obtained in magnetic resonance imaging (MRI). In patients with poor kidney function - such as those suffering from chronic kidney disease - Gd(III)-based contrast agents can lead to serious problems such as contrast-induced nephropathy [1] and nephrogenic systemic fibrosis (NSF) [2, 3], which can both cause renal failure. This arises because high doses of Gd-based contrast agents are required to obtain good quality images.

To ameliorate these issues, manganese species have been explored as alternative contrast agents. The similarity of the ionic radii of Ca^{2+} and Mn^{2+} means that Mn^{2+} can effectively compete with Ca^{2+} in many biological systems, and the uptake of Mn^{2+} can allow the tracking and visualization of both the healthy and diseased central nervous system [4, 5]. That said, caution is required because high-dose manganese accumulated within the human body, especially in the brain, can cause a form of Parkinsons's disease (manganism) [6-8].

The Mn(II) complexes typically used are chelates such Mn(EDTA)(H_2O) (Mangascan, Mn(II) ethylenediaminetetraacetate) and Mn(DPDP) (Teslascan, Mn(II) dipyridoxal diphosphate). A range of Mn aminophosphonate complexes has also been reported [9], and found to have higher affinity for calcified tissues than aminocarboxylate complexes. In addition, the analogous gadolinium aminophosphonate complexes have previously been found to bind strongly to hydroxyapatite (one of the major constituents of bone) [10].

The aim of chelation is to prevent the release of free Mn ions into the body, but the low molecular weight species described above can lose Mn(II) relatively easily, and dechelated Mn(II) ions can accumulate and lead to toxicity [11]. To preclude this, the immobilization of the ions into larger systems has been proposed. Several studies have explored this, for instance by incorporating MnO into colloidal particles [12, 13] and mesoporous silica [14]. Mn(II) chelates have additionally been immobilized onto a dendrimer structure [15].

Here, we adopted a different approach to prevent leaching. Many of the Mn(II) complexes which can be used for MRI imaging – including the Mn aminophosphonates – are capable of forming anions. They can thus be loaded into solid state matrices by the technique of ion exchange. There exists a range of layered

metal hydroxide (LMH) systems which have positively charged metal hydroxide layers and interlayer anions which can be easily replaced by ion exchange, and these were selected as host materials. One such family of materials, the layered double hydroxides (LDHs, which typically contain a mixture of divalent and trivalent metal cations) has formed the focus of several relevant investigations. In these, researchers intercalated anionic contrast agents into the LDHs and found the resultant composites to possess increased relaxivity [16] [17].

Hydroxy double salts (HDSs) comprise another family of LMHs, and have been much less explored than LDHs: we are not aware of any reports investigating them for use in MRI. They have the general formula $[(M^{2+}_{1-x}M'^{2+}_{1+x})(OH)_{3(1-y)}]X^{n-}_{(1+3y)/n}\cdot zH_2O$, where M^{2+} and M'^{2+} are divalent metals and X^{n-} is an exchangeable anion [18]. Here, we used the biocompatible $[Zn_5(OH)_8]Cl_2\cdot yH_2O$ (Zn_5-Cl) HDS as a host material. We first synthesized and characterized a range of Mn(II) aminophosphonate complexes (MnL^1, MnL^2, MnL^3 and $Mn_2L^4_2$; see Figure 1). We then intercalated these into Zn_5-Cl. Finally, the proton relaxation properties of both the raw complexes and the complex-HDS composites were evaluated.

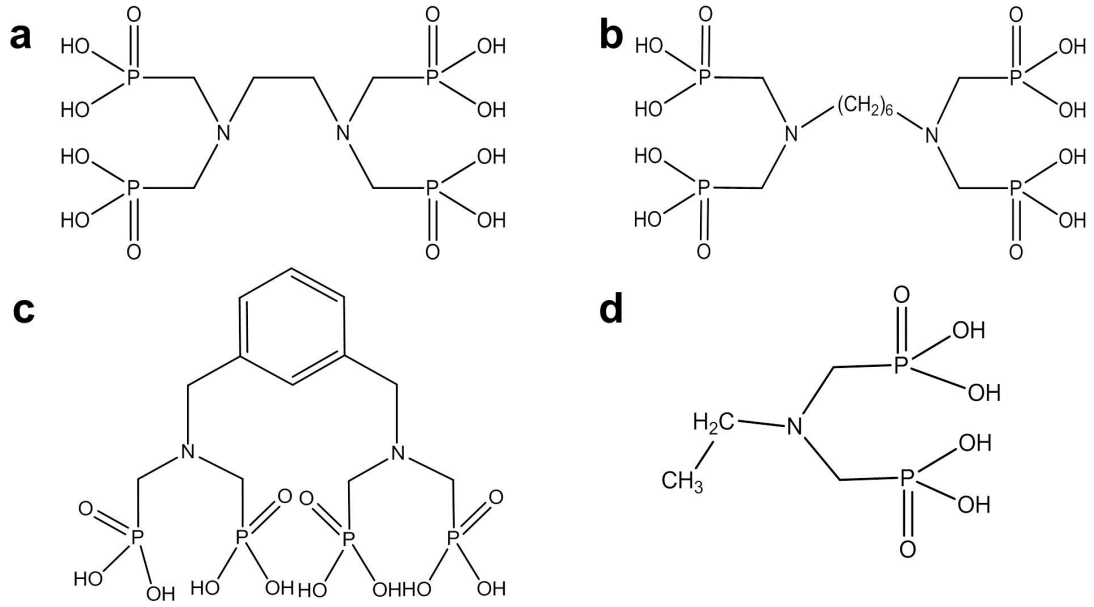

Figure 1: The chemical structures of the ligands used in this work. (a) ethylene diamine tetra(methylene phosphonic acid (L^1), (b) hexamethylene diamine tetra(methylene phosphonic acid) (L^2), (c) xylene diamine tetra(methylene phosphonic acid) (L^3), and (d) amino ethyl dimethylene phosphonic acid (L^4).

2. Materials and methods

2.1 Materials

Zinc chloride, zinc oxide and manganese (II) oxide were obtained from Sigma-Aldrich UK. Sodium hydroxide tablets were procured from Fisher Scientific UK. All water used was de-ionised prior to use. L^1, L^2 L^3 and L^4 were prepared according to the literature method [10].

2.2 Methods

2.2.1 Synthesis of $[Zn_5(OH)_8]Cl_2{\cdot}yH_2O$

The HDS ($[Zn_5(OH)_8]Cl_2{\cdot}yH_2O$) was prepared by the reaction of 7.26 g (0.053 mol) $ZnCl_2$ and 3.00 g (0.037 mol) of ZnO in 18 ml deionized water. The dispersion was stirred vigorously at room temperature for 7 days. The solid product was recovered by vacuum filtration and washed with water. Finally the solid product was dried in air.

2.2.2 Synthesis of Mn(II) aminophosphonates [MnL^1, MnL^2, MnL^3, $Mn_2(L^4)_2$]

MnL^1, MnL^2, MnL^3 and $Mn_2(L^4)_2$ were prepared through reaction of the polyaminophosphonate ligand and MnO (molar ratio 1 : 1). This process mirrors the literature precedent for the analogous Gd(III) materials, but using MnO instead of Gd_2O_3 [9, 10].

The successful formation of the Mn aminophosphonate complexes was verified by elemental analysis and IR spectroscopy (Table 1).

Table 1: Elemental analysis and IR data for the Mn complexes prepared in this work.

ID	Formula	Elemental contents / % Obsd. (calcd.)[a]	Vibrational frequency (P=O/P-OH) / cm^{-1}
MnL^1	$Mn(C_6H_{18}N_2P_4O_{12})(H_2O)_{1.5}$	C: 14.61 (13.96) H: 3.81 (4.10) N: 5.61 (5.43) H_2O: 5.09 (5.24)	1139, 1047, 934
MnL^2	$Mn(C_{10}H_{26}N_2P_4O_{12})(H_2O)_{1.3}$	C: 21.87 (21.12) H: 4.68 (5.07) N 5.19 (4.93) H_2O: 4.16 (4.12)	1149, 1057, 907
MnL^3	$[Mn(C_{12}H_{22}N_2P_4O_{12})(H_2O)_{1.9}][MnO]_{1.5}$	C: 20.35 (20.72) H: 3.42 (3.68) N: 4.31 (3.97) H_2O: 4.93 (4.85)	1153, 1083, 917
$Mn_2(L^4)_2$	$Mn_2(C_4H_{11}NP_2O)_2(H_2O)_{1.5}$	C: 15.43 (15.34) H: 4.33 (4.51) N: 4.57 (4.47) H_2O: 8.47 (8.63)	1183, 1050, 917

[a] C, H, and N contents were determined by elemental microanalysis, and the water content estimated from thermogravimetric analysis assuming that the first stage of mass loss arose from dehydration. The stages of mass loss were not always clear however, and thus some uncertainty surrounds these numbers.

2.2.3 Ion exchange intercalation

The $[Zn_5(OH)_8]Cl_2{\cdot}yH_2O$ (Zn_5-Cl) host material (0.2 mmol) was suspended in 5 mL of an aqueous solution containing 0.04 mmol of a Mn complex (L^1, L^2, L^3 and $(L^4)_2$) and 0.08 mmol (a two-fold molar excess with respect to Mn) of NaOH. The suspension was stirred at 60 °C for 7 days. The resultant suspension was transferred to a centrifuge tube and spun at 2000 rpm for 6 minutes. The supernatant was discarded. The solid was washed with water, re-suspended and centrifuged again, with this process repeated in total three times. The solid product was dried in an oven at approximately 30 °C for 24 h. To explore the effect of the reaction parameters, additional samples were prepared with variations in the amount of Mn complex (0.04, 0.08, 0.12 mmol) and volume of water used (1, 2, 5, 10 mL). All other reaction conditions were kept constant.

2.3 Characterization

2.3.1 Powder X-ray diffraction

X-ray diffraction patterns were recorded over the 2θ range from 3.5 to 40 °on a powder diffractometer (PW 1830/40, Philips, Amsterdam, Netherlands) using Cu Kα radiation at 40 kV and 25 mA.

2.3.2 Fourier transform infrared (FTIR) spectroscopy

FTIR analyses were carried out on a Spectrum 100 instrument (PerkinElmer Co. Ltd, Waltham, MA, USA) over the range 650 – 40000 cm^{-1} at a resolution of 4 cm^{-1}.

2.3.3 Thermogravimetric analysis

Thermogravimetric analysis (TGA) was undertaken with the aid of a Discovery analyser (TA Instruments, New Castle, DE, USA). Approximately 3 – 4 mg of a sample was loaded into an open aluminium pan and then heated at 10 °C min^{-1} from 30 to 300 °C. Experiments took place under a flow of N_2 gas (25 mL min^{-1}).

2.3.4 Elemental microanalysis

C, H, and N contents were determined using the combustion method on a Flash 2000 Elemental Analyser (Thermo Scientific, Waltham, MA, USA).

2.3.5 Microwave plasma-atomic emission spectroscopy

The Mn content of the intercalation compounds was determined by microwave plasma-atomic emission spectroscopy (MP-AES; 4100 instrument, Agilent Technologies, Santa Clara, California, USA). 10 mg of the sample was placed in a 50 mL volumetric flask and digested in diluted nitric acid (0.5 %). Mn emission was measured for the lines at 257.610 [Mn(II)], 259.372 [Mn(II)], and 403.076 nm [Mn(I)]. Calibration was performed over the range is 1.56 – 100 ppm.

2.3.6 X-ray fluorescence

The Zn : Mn ratio in the intercalates was determined for selected samples using

X-ray fluorescence (XRF). Samples were finely ground before measurement and placed onto clingfilm. A glass slide was used to flatten the powders, and the samples were then placed onto the fluorimeter (X-Met 3000TXR+, Oxford Instruments, Abingdon, UK) for measurement.

2.3.7 *In vitro* release studies

Approximately 10 mg of the intercalation compound was placed in 20 mL of a phosphate buffered saline (PBS; pH 7.4) buffer and incubated at 37 °C under stirring at 100 rpm. 10 mL aliquots were withdrawn from the buffer at predetermined time points and replaced by 10 mL of fresh buffer to maintain a constant volume. The aliquots were centrifuged (2000 rpm, 6 minutes; 5804R centrifuge, Eppendorf, Hauppauge, NY, USA) and the Mn complex content in the resultant supernatant quantified by UV-vis spectroscopy (Cary 100 spectrophotometer, Agilent Technologies, Santa Clara, California, USA). Each experiment was repeated three times, and results are reported as mean ± S.D.

2.3.8 Proton relaxivity measurements

Measurements of the longitudinal (T_1) and transverse (T_2) relaxation times of water protons were carried out on a Bruker Minispec mq20 relaxometer (20 MHz, 0.47 T, Bruker Corporation, Billerica, MA, USA) at 37 °C, using inversion recovery and CPMG pulse sequences, respectively. 5 mg of the sample was placed in a 10 mm-diameter NMR tube and held using 1 mL of 1% agarose.

3. Results

3.1 X-ray diffraction

XRD patterns for the Zn_5-Cl HDS and the intercalation compounds Zn_5-MnL^1, Zn_5-MnL^2, Zn_5-MnL^3 and Zn_5-$Mn_2(L^4)_2$ are shown in Figure 2. Clear evidence of partial intercalation can be seen.

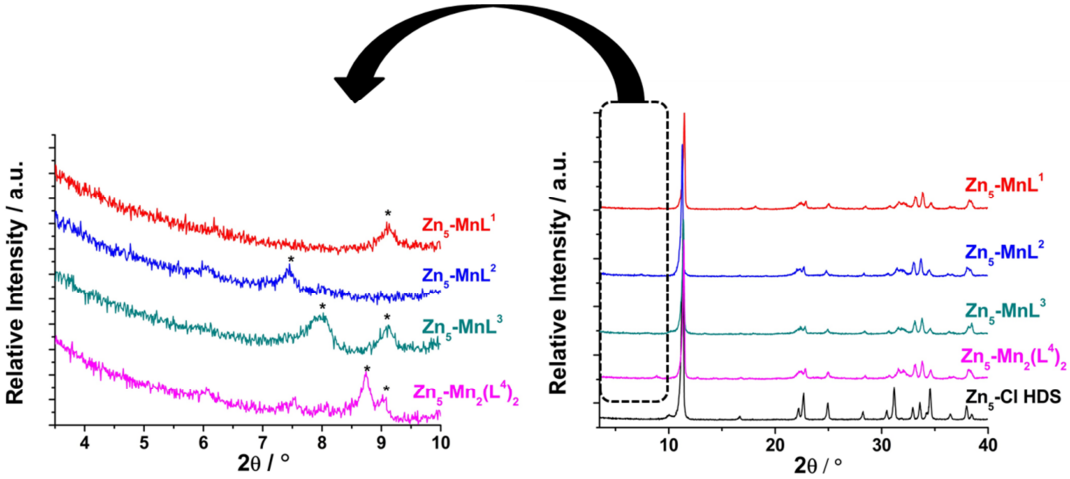

Figure 2: X-ray diffraction patterns of Zn_5-MnL^1, Zn_5-MnL^2, Zn_5-MnL^3, Zn_5-$Mn_2(L^4)_2$, with the intercalate reflections marked *.

The interlayer spacing in the Zn_5-Cl HDS is 7.8 Å. After reaction with Mn complexes, the most intense reflections become broader and less intense compared with the pristine Zn_5-Cl material, suggesting partial intercalation of the complexes in some interlayer spaces. In addition, a new set of weak Bragg reflections emerges at lower angle. These arise over the angular range from *ca*. 9 to *ca*. 10° for Zn_5-MnL^1, 7.5° for Zn_5-MnL^2, 8.1/ 9.1° for Zn_5-MnL^3 and 8.8 / 9.1° for Zn_5-$Mn_2(L^4)_2$. These reflections are marked * in Figure 2. These reflections correspond to an increase in the interlayer spacing to 10 - 12 Å. These reflections are attributed to the formation of Zn_5-complex intercalates. Notably, there are two distinct sub-10° reflections in Zn_5-MnL^3 and Zn_5-$Mn_2(L^4)_2$, as detailed in Table 2. This may be caused by the adoption of different arrangements of $[MnL^3]^{2-}$ and $[Mn_2(L^4)_2]^{2-}$ in the interlayer regions. In all the patterns of Mn chelate-loaded HDSs, a reflection corresponding to unexchanged chloride appears at *ca*. 11°.

Table 2: X-ray diffraction data for Zn_5-Mn complex.

Sample	Reaction molar ratio Zn_5-Cl : Mn complex	1st guest	d_{003} / Å	2nd guest	d_{003} / Å
Zn_5-MnL^1	5 : 1	$[MnL^1]^{2-}$	9.7	Cl^-	7.7
Zn_5-MnL^2	5 : 1	$[MnL^2]^{2-}$	11.9	Cl^-	7.8
Zn_5-MnL^3	5 : 1	$[MnL^3]^{2-}$	9.7 / 11.2	Cl^-	7.8
Zn_5-$Mn_2(L^4)_2$	5 : 1	$[Mn(L^4)_2]^{2-}$	9.7 / 10.1	Cl^-	7.8

3.2 IR spectroscopy

The IR spectra of the intercalation compounds are presented in Figure 3.

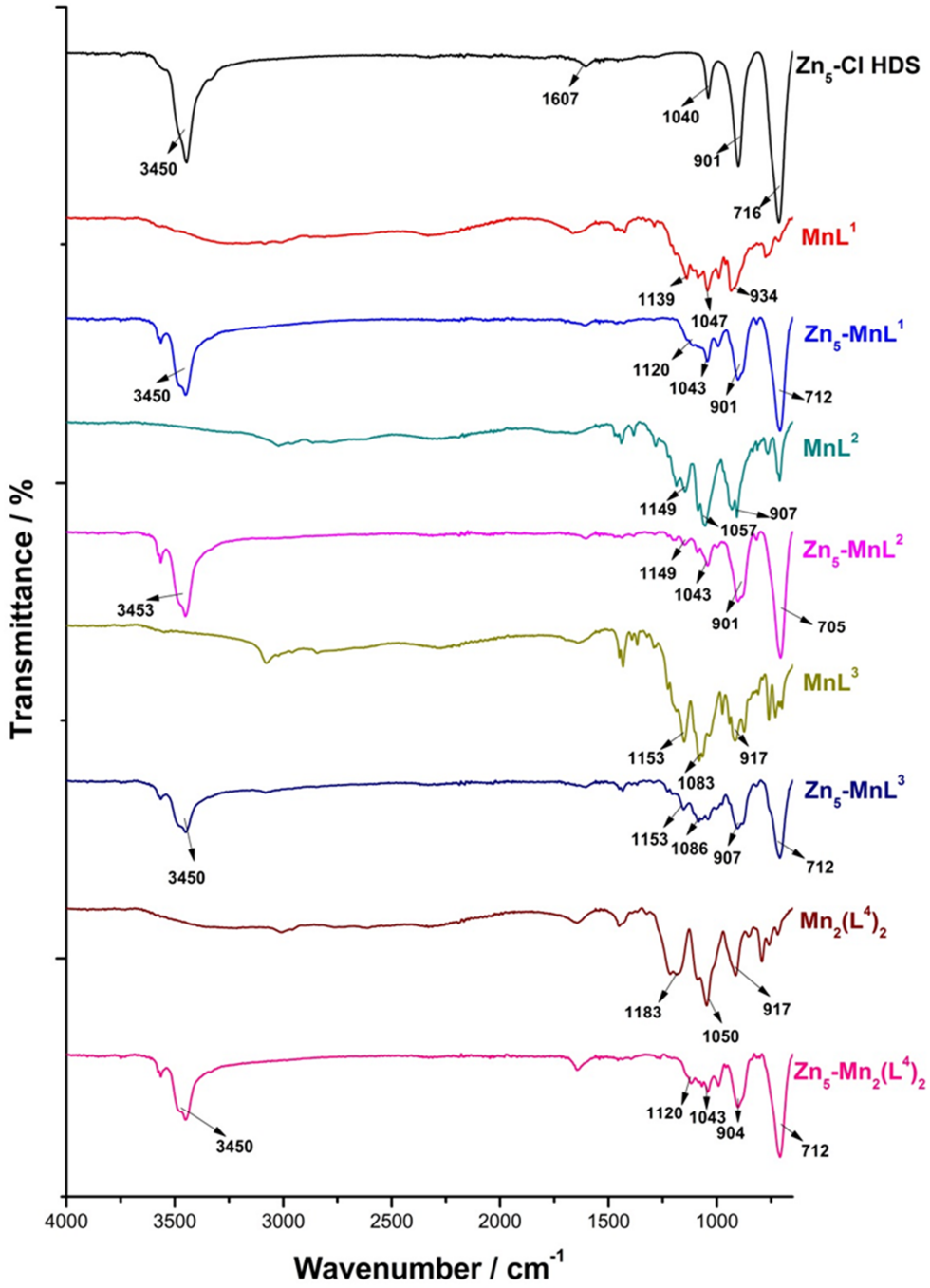

Figure 3: IR spectra of Zn_5-Cl HDS, Zn_5-MnL^1, Zn_5-MnL^2, Zn_5-MnL^3, and Zn_5-$Mn_2(L^4)_2$, together with those of the unreacted complexes.

The intense band located at 3450 cm^{-1} in the spectrum of Zn_5-Cl is associated with stretching vibrations of OH groups in the layers. A small water absorption band (originating from the delta bend) is at 1607 cm^{-1}. The bands below 1040 cm^{-1} are attributed to Zn-O vibrational bending.

Characteristic PO_3 bands can be seen in the region of 1200 cm^{-1} – 900 cm^{-1} after the Mn complexes are incorporated into Zn_5-Cl, confirming their successful intercalation. These peaks shift from 1047/934 cm^{-1} (v(P=O), v(P-O(H))) in MnL^1 to 1043/901 cm^{-1} in Zn_5-MnL^1, 1057/907 cm^{-1} in MnL^2 to 1043/901 cm^{-1} in Zn_5-MnL^2, 1083/917 cm^{-1} in MnL^3 to 1086/907 cm^{-1} in Zn_5-MnL^3 and 1050/917 cm^{-1} in $Mn_2(L^4)_2$ to 1043/904 cm^{-1} in Zn_5-$Mn_2(L^4)_2$ due to electrostatic and hydrogen bonding interactions between the P=O groups and HDS layers.

3.3 Elemental analysis

XRF data were used to determine the Zn : Mn ratio in the intercalates: the results are shown in Table 3. The Mn(II) complex contents were calculated to be approximately 10 wt% in the composites.

Table 3: XRF data for Mn complex intercalates

Sample	Zn : Mn molar ratio	Proposed formula
Zn_5-MnL^1	5 : 0.069	$[Zn_5(OH)_8]Cl_{1.862}(MnC_6H_{17}N_2P_4O_{12})_{0.069}\cdot 2H_2O$
Zn_5-MnL^2	5 : 0.079	$[Zn_5(OH)_8]Cl_{1.842}(MnC_{10}H_{26}N_2P_4O_{12})_{0.079}\cdot 2H_2O$
Zn_5-MnL^3	5 : 0.074	$[Zn_5(OH)_8]Cl_{1.852}(MnC_{12}H_{22}N_2P_4O_{12})_{0.074}\cdot 2H_2O$
Zn_5-$Mn_2(L^4)_2$	5 : 0.063	$[Zn_5(OH)_8]Cl_{1.936}\ (Mn_2(C_4H_{11}NP_2O_6)_2)_{0.032}\cdot 2H_2O$

3.4 Mn(II) complex release

Zn_5-MnL^3 was taken as an examplar system to explore the rate of complex release from the intercalates. The UV-vis spectrum of MnL^3 shows absorbances at 209 and 248 nm, while those of L^3 and its dianion contain peaks at 212 / 265 nm and 211 / 265 nm respectively. Analysis of the release aliquots reveals that absorbance peaks arise at 207 and 247 nm. There is no absorbance at 265 nm (data not shown). It is thus clear that the entity released is the MnL^3 complex, and that there is no separation of the Mn(II) ion and the ligand.

Having established this, the release of MnL^3 from Zn_5-MnL^3 was quantified as a function of time using the peak at 247 nm (Figure 4).

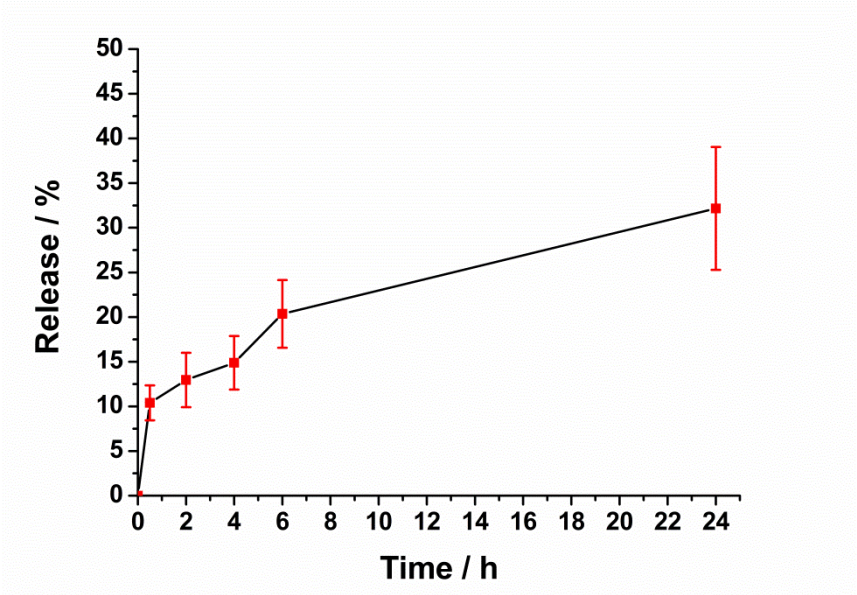

Figure 4: The release profile of MnL^3 from Zn_5-MnL^3. Data are shown as mean ± S.D. from three independent experiments.

There is initially a burst of release of MnL^3 (ca. 20 %) from the complex during the first 6 h of the experiment. This is followed by more gradual release reaching ca. 30 % after 24 h. These findings are very similar to those found in the literature for Gd complex intercalates of HDSs [19]. The burst effect is attributed to the external adsorption of some Mn(II) complex on the HDS surface. The subsequent release is thought to result from ion-exchange between the anions in the interlayer and phosphate anions in the buffer. This is a much slower process than release from the surface due to the strong electrostatic interactions which exist between the HDS layer and the MnL^3 complex. Given that only 30 % of the incorporated Mn(II) complex is freed after 24 h, it is thus clear that the intercalates have a high degree of stability under physiological conditions, and Mn(II) leakage is not a significant concern.

3.5 Proton relaxivities

The longitudinal (r_1) and transverse (r_2) relaxivities (relaxation rate enhancement per mM metal ion concentration) of the Mn(II) complex intercalates, together with controls, are listed in Table 4.

Table 4: Proton relaxivities of the Mn complexes and their intercalates.

Sample	[Mn] /mM	T_1 / ms	T_2 / ms	r_1 / $s^{-1}mM^{-1}$	r_2 / $s^{-1}mM^{-1}$
Agarose gel		3200.00 ± 100	107.00 ± 2.00		
Zn_5-Cl		3000.00 ± 10.0	140.00 ± 2.00		
MnL^1	1.00	380.23 ± 1.21	56.15 ± 0.13	2.63 ± 0.02	17.81 ± 0.05
MnL^2	1.00	303.95 ± 1.71	50.18 ± 0.08	3.29 ± 0.03	19.93 ± 0.03
MnL^3	1.13	454.13 ± 0.42	57.77 ± 0.05	1.95±0.002	15.32 ± 0.01
$Mn_2(L^4)_2$	0.74	87.80 ± 0.26	15.11 ± 0.04	15.39±0.05	89.41 ± 0.24
Zn_5-Cl + MnL^1 [a]	1.00	666.67 ± 0.49	62.66 ± 0.05	1.50±0.003	15.96 ± 0.01
Zn_5-Cl + MnL^2 [a]	1.00	1960.78 ± 5.00	75.38 ± 0.40	0.51±0.002	13.27 ± 0.04
Zn_5-Cl + MnL^3 [a]	1.00	1449.30 ± 2.04	81.07 ± 0.35	0.69±0.01	12.32 ± 0.005
Zn_5-Cl +$Mn_2(L^4)_2$ [a]	0.90	99.62 ± 0.80	17.56 ± 0.08	11.1± 0.09	63.26 ± 0.28
Zn_5-MnL^1	0.83	1019.83 ± 13.20	69.32 ± 0.07	1.19 ± 0.02	17.43 ± 0.02
Zn_5-MnL^2	0.92	1369.50 ± 2.12	72.22 ± 0.06	0.79 ± 0.46	15.02 ± 0.01
Zn_5-MnL^3	1.00	1479.50 ± 2.12	91.98 ± 0.16	0.67 ± 0.40	10.85 ± 0.02
Zn_5-$Mn_2(L^4)_2$	0.35	265.20 ± 0.20	48.43 ± 0.02	10.8±0.004	58.99 ±0.004

[a] These materials are physical mixtures of the two components.

Relaxivities were obtained by measuring the paramagnetic longitudinal and transverse relaxation times and comparing these to the Mn concentrations (determined through microwave plasma-atomic emission spectroscopy). The relaxation times of the diamagnetic Zn_5-Cl HDS (T_1 = 3000 ms, T_2 = 140 ms) and agarose gel (T_1 = 3200 ms, T_2 = 107 ms) when compared to those of water (T_1 = 2700 ms, T_2 = 3400 ms) show no change in the water proton T_1 relaxation process. There is a small but non-negligible decrease of T_2 due to the relative immobilization of water molecules in the diamagnetic agarose gel and at the surface of the Zn_5-Cl HDS.

The proton relaxivities of paramagnetic metal complexes may result from inner-sphere, second-sphere and outer-sphere contributions [20, 21]. The number of water molecules in the first hydration sphere is very important in determining the

size of the inner-sphere contribution. However, the contribution of water molecules present for long lifetimes in the second-sphere of complexes can also be significant [22, 23]. This is particularly true for polyaminophosphonate complexes, due to hydrogen bonding of water molecules with the phosphonate oxygens [24]. This effect is even more noticeable in phosphonate complexes with no inner-sphere water, such as $Gd(DOTMP)^{5-}$ (DOTMP = 1,4,7,10-tetraazacyclododecane-1,4,7,10-tetrakis(methylphosphonic acid) and other Gd(II) tetraazaphosphonate and phosphinate complexes [25].

Oakes *et al.* have developed a method to determine the number of inner sphere water molecules (q) from water proton relaxation rates (r_1) of aqueous solutions of paramagnetic complexes [26]. Assuming that Mn^{2+}(aq) has a q value of 6, a value of q = 0.99 was obtained for$[Mn(EDTA)]^{2-}$, indicating that in solution the coordination sphere of Mn^{2+} is expanded to a coordination number of 7, with one inner-sphere water molecule [26]. This observation was in agreement with the X-ray crystal structure of the same complex [27] and further confirmed by proton nuclear magnetic relaxation dispersion studies [28]. The same technique was applied to MnL^1, giving a value of q = 1.20; this was corrected to q = 1.32 or 1.44 assuming one or two unbound phosphonate groups at a time [26]. However this latter calculation might overestimate the q value, as it did not take into account the possible contribution of second sphere relaxation.

We found that MnL^1 has 2.63 $mM^{-1}s^{-1}$ for r_1 and 17.81 $mM^{-1}s^{-1}$ for r_2 at 20 MHz and 37 °C (Table 4). The former is very similar to the reported r_1 value of the analogous $[Mn(EDTA)(H_2O)]^{2-}$ species (2.9 $s^{-1}mM^{-1}$ at 20 MHz, 37 °C) which has q = 1 and a negligible second sphere relaxation contribution [29, 30]. Taking into account the significant second-sphere contribution expected, our results for MnL^1 point to a q value between 1 and 0. This is less than the water content observed by TGA, but it is very likely that not all the water evolved during heating is present in the inner sphere

of Mn(II).

The increase in the length of the linear aliphatic chain connecting the N atoms going from L^1 to L^2 (Figure 5) slightly increased the relaxivities of the MnL^2 complex (to r_1 = 3.29 $mM^{-1}s^{-1}$, r_2 = 19.93 $mM^{-1}s^{-1}$). This is probably due, in part, to the increased size of the compound leading to a slower tumbling time [9].

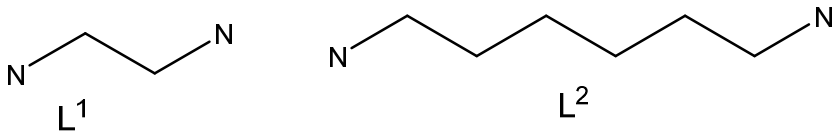

Figure 5: The aliphatic chains connecting the N atoms in L^1 and L^2.

However, the structure of the L^2 ligand is such that steric hindrance may prevent the simultaneous co-ordination of all six donors groups to the metal ion, increasing the value of q, which also would contribute to the observed r_1 increase. This is in agreement with the observation that MnL^2 is less stable than MnL^1 [31]. The complex structure proposed in the literature (see Figure 6) for the complex with only two nitrogen atoms and one phosphonate group chelated to Mn(II) forming a stable cyclic structure is highly improbable, as it would imply a q value too high to be compatible with the observed r_1 [31].

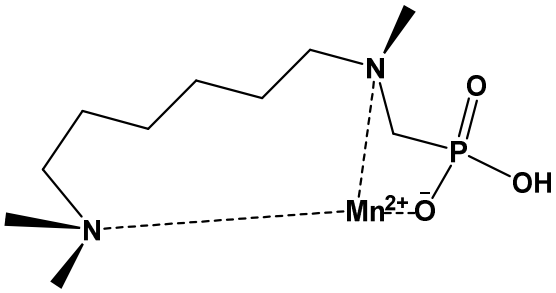

Figure 6: The proposed cyclic structure of MnL^2.

There is evidence that aminophosphonate ligands with two or more phosphonate groups have lower coordination tendencies than expected due to the mutual

repulsion between adjacent binegative phosphonate groups [32, 33]. This is reflected in the stability constants of the MnL^1 and MnL^2, which are smaller than those of the corresponding carboxylate analogues EDTA and HDTA [31]. Therefore, the tendency to have some unbound phosphonate group may increase as their number increases in the ligand, with the resultant possibility of higher q values.

MnL^3 has previously been reported to have better relaxation than MnL^1 at 10 MHz and 37 °C (10 mM^{-1} s^{-1} *vs.* 3.7 $mM^{-1}s^{-1}$), thought to be because the introduction of the aromatic ring increased the molecular weight [9]. However, in this work, at 20 MHz and 37 °C MnL^1 (r_1 = 2.63 $mM^{-1}s^{-1}$) gives faster relaxation than MnL^3 (r_1 = 1.95 $mM^{-1}s^{-1}$). This can be explained because the steric crowding of MnL^3 prevents the binding of inner water or restricts the exchange of bound water protons [34].

Among the four Mn complexes, $Mn_2(L^4)_2$ shows the most effective relaxation. This is believed to be a result of it having a flexible structure (see Figure 7). This structure can lead to the wrapping of two Mn^{2+} ions by two L^4 ligands, with a bridging water molecule, giving a coordination number of six for each Mn. This structure is consistent with the elemental analysis and TGA data. It is thought to give an increased number of inner sphere water molecules and therefore leads to the increased relaxivities attained.[34]

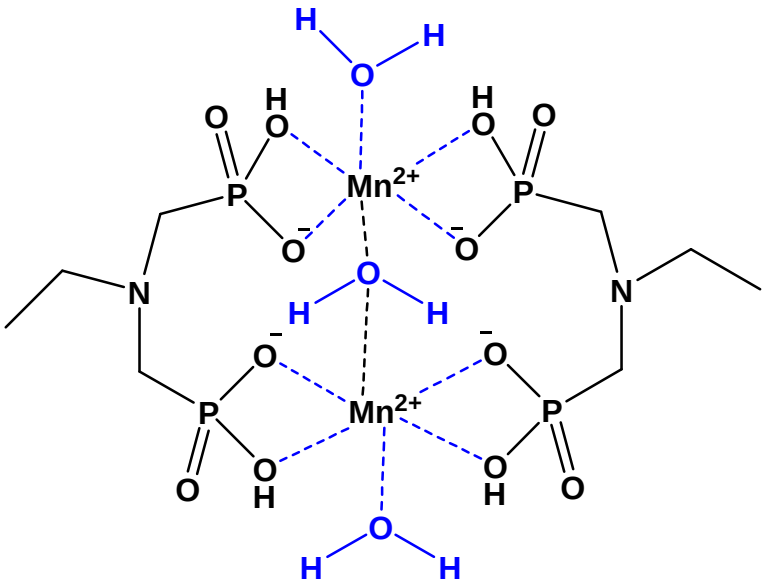

Figure 7: The proposed structure of $Mn_2(L^4)_2$.

The analogous Gd complexes have previously been studied in detail at 10 MHz and 37 °C [10]. The Mn complexes generally have lower values for r_1 but slightly higher values for r_2: GdL^{1-} had $r_1 = 11.1\ mM^{-1}s^{-1}$ and $r_2 = 15.9\ mM^{-1}s^{-1}$, while GdL^3 showed $r_1 = 10.0\ mM^{-1}s^{-1}$ and $r_2 = 14.3\ mM^{-1}s^{-1}$ (at 10 MHz and 37 °C) [10]. This is expected to arise because there is a much more important scalar contribution to r_2 in the case of Mn(II) complexes, while the scalar contribution to r_1 is very small, especially for Gd(III) complexes (where dipole-dipole interactions are dominant) [20, 21]. Such a scalar contribution to r_2 increases drastically at high magnetic fields due to the field dependence of the electron spin relaxation time (τ_S), which rises sharply at high fields. In addition, the presence of a non-dispersive τ_S term in the equation for the contact relaxation causes r_2 to become proportional to τ_S at high fields, and thus to increase steadily [20].

The Mn complex intercalates showed lower relaxivities than their physical mixture counterparts (see Table 4Table 4). These decreased relaxivities probably result from reduced hydration numbers. Steric compression in the interlayer might eliminate water molecules from the inner coordination sphere, meaning that in the intercalates

no water molecule is directly coordinated to the Mn complexes [35]. Low longitudinal relaxivities could arise from co-intercalated chloride ions exchanging with water molecules bound to Mn(II). In addition, HDSs have very high affinity for carbonate ions, and thus small amounts of dissolved carbon dioxide can lead to the incorporation of CO_3^{2-} into the interlayer space. This too could displace inner sphere water molecules from the Mn complexes.

3.6 Variation of intercalation conditions

In attempts to enhance the relaxivity, a number of experiments were performed in which the intercalation conditions were systematically varied. The molar ratio of Zn_5-Cl to Mn complex was varied from 5:1 to 5:2 and 5:3, and the volume of water used for experiments changed from 5 mL to 10, 2, and 1 mL. This led to a series of 12 intercalates for each complex.

In general, there is no noticeable effect of varying the HDS : guest ratio or the amount of water used for reaction on the interlayer spacing or the extent of reaction (see Supplementary Information Tables S1 to S4). The exception to this is with MnL^1, where intercalation could only be clearly seen for the sample reported above. Taking Zn_5-MnL^2 as an example (Figure 8), it is clear that changing the volume of water used does not affect the crystallinity of the product. Increasing the amount of guest used in the reactions (e.g. going from a 5:1 to 5:3 molar ratio) does in some cases result in an increase in the intensity of the intercalate reflection, but this is not a universal observation.

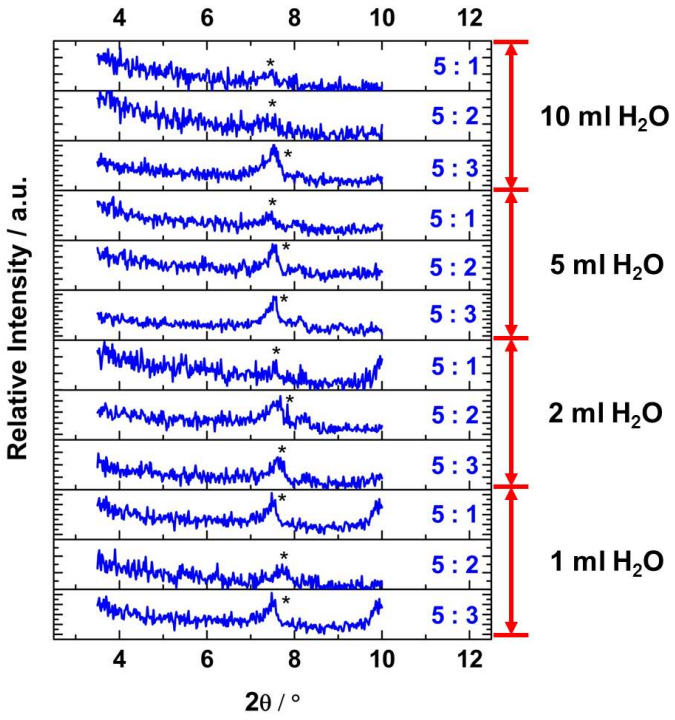

Figure 8: The effect of varying the reaction parameters on the low-angle XRD patterns of Zn_5-MnL^2 intercalates. The ratio indicated is the HDS : Mn complex ratio used for intercalation.

The similarity of the intercalation compounds, regardless of the guest excess and water volume used, is reflected in their r_1 and r_2 values (see Table S5), which are all relatively similar. These are illustrated in Figure 9. It can be seen that there are no major trends resulting from variation in reaction parameters. In terms of the r_1 values, the Zn_5-$Mn_2(L^4H_1)_2$ systems give continually higher values than the Zn_5-$Mn(L^3H_4)$ or Zn_5-$Mn(L^2H_4)$ materials, with a maximum value of 17.12 $mM^{-1}s^{-1}$. There are no clear trends in the r_2 data, but from a suitable choice of parameters it is possible to obtain r_2 values as high as 68.31 $mM^{-1}s^{-1}$. This r_1 value is two-fold higher than that reported for a Mn(II)-based dendrimer containing six tyrosine-derived $[Mn(EDTA)(H_2O)]^{2-}$ units conjugated with a cyclotriphosphazene core (r_1 = 8.2 $s^{-1}mM^{-1}$ at 20 MHz).[15]

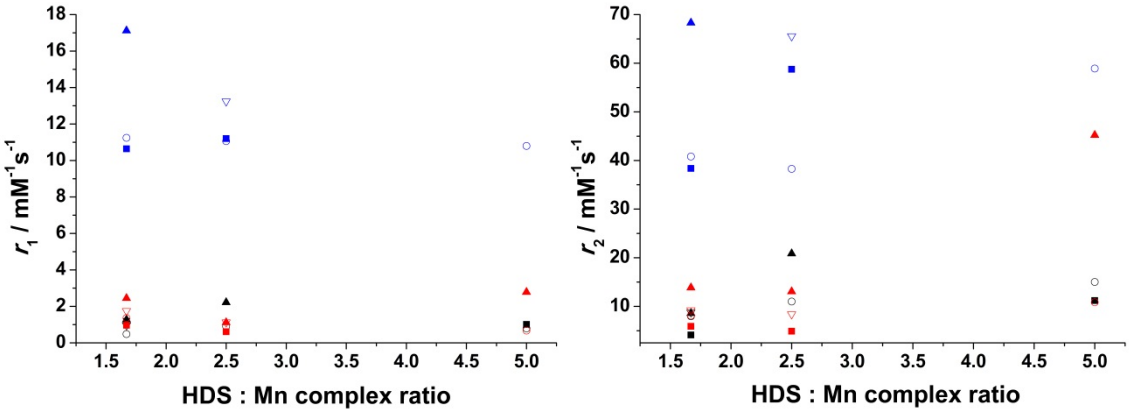

(a) (b)

Figure 9: The (a) r_1 and (b) r_2 values obtained for the Mn complex intercalates as a function of reaction conditions. Symbols are as follows: ■ Zn_5-MnL^2, 10 mL water; ○ Zn_5-MnL^2, 5 mL water; ▲ Zn_5-MnL^2, 2 mL water; ▽ Zn_5-MnL^2, 1 mL water; ■ Zn_5-MnL^3, 10 mL water; ○ Zn_5-MnL^3, 5 mL water; ▲ Zn_5-MnL^3, 2 mL water; ▽ Zn_5-MnL^3, 1 mL water; ■ Zn_5-$Mn_2(L^4)_2$, 10 mL water; ○ Zn_5-$Mn_2(L^4)_2$, 5mL water; ▲ Zn_5-$Mn_2(L^4)_2$, 2 mL water; ▽ Zn_5-$Mn_2(L^4)_2$, 1 mL water.

The results observed here in general accord well with the literature. The incorporation of MnO into colloidal particles [12] and mesoporous silica [14] also resulted in low relaxivities (r_1 = 0.37 $s^{-1}mM^{-1}$ and r_2 = 1.74 $s^{-1}mM^{-1}$; r_1=0.99 $s^{-1}mM^{-1}$ and r_2 = 11.02 $s^{-1}mM^{-1}$ respectively). Nevertheless, the previously reported systems still showed the ability to selectively enhance breast cancer cells in T_1-weighted MRI [12], or to label and track mesenchymal stem cells [14]. Thus, it seems likely that the Mn complex / HDS composites prepared in this work will also have utility as contrast agents. The advantage of the HDS-based materials is that the embedded Mn(II) is chelated (unlike the MnO systems), and therefore they are expected to have much reduced toxicity.

4. Conclusions

A series of Mn(II) chelation complexes was synthesised and fully characterized. They were subsequently loaded into the hydroxy double salt (HDS) $[Zn_5(OH)_8]Cl_2{\cdot}2H_2O$ (Zn_5-Cl). Successful preparation of HDS/Mn chelate composites was confirmed by X-ray diffraction, IR spectroscopy, X-ray fluorescence (XRF), and microwave plasma-atomic emission spectroscopy (MP-AES). The interlayer spacing was observed

to increase from 7.8 Å with Zn_5-Cl HDS to 10 – 12 Å for the intercalates. The characteristic absorption bands of the Mn(II) complexes were clearly visible in the IR spectra of the intercalates, indicating the encapsulation of intact Mn(II) complexes in the Zn_5-HDS. The presence of Mn was unequivocally demonstrated by XRF and MP-AES measurements. The longitudinal relaxivities of the complexes after intercalation showed somewhat lower values compared with the pure complexes and physical mixtures of the complexes and HDS, probably because of steric crowding and/or carbonate exchange leading to no inner-sphere water being bound to the Mn(II) centre. Nevertheless, the r_1 and in particular the r_2 values are still sufficient to give the HDS/Mn complex composites potential utility as contrast agents.

5. Acknowledgements

CFGCG would like to thank the FCT-Portugal (Portuguese Foundation for Science and Technology) and FEDER–European Regional Development Fund through the COMPETE Programme (Operational Programme for Competitiveness) for funding (UID/QUI/00313/2013 and PEst-OE/QUI/UI0313/2014).

6. References

[1] S.R. Walsh, T. Tang, M.E. Gaunt, J.R. Boyle, J. Endovasc. Ther., 14 (2007) 92.

[2] L. Yang, I. Krefting, A. Gorovets, L. Marzella, J. Kaiser, R. Boucher, D. Rieves, Radiology, 265 (2012) 248.

[3] J. Perez-Rodriguez, S. Lai, B.D. Ehst, D.M. Fine, D.A. Bluemke, Radiology, 250 (2009) 371.

[4] I. Aoki, C. Tanaka, T. Takegami, T. Ebisu, M. Umeda, M. Fukunaga, K. Fukuda, A.C. Silva, A.P. Koretsky, S. Naruse, Magnet. Reson. Med., 48 (2002) 927.

[5] N.A. Bock, A.C. Silva, Future Neurol., 2 (2007) 297.

[6] J. Crossgrove, W. Zheng, NMR Biomed., 17 (2004) 544.

[7] M. Aschner, K.M. Erikson, D.C. Dorman, Critical Rev. Toxicol., 35 (2005) 1.

[8] M.G. Cersosimo, W.C. Koller, Neurotoxicology, 27 (2006) 340.

[9] C.T. Harding, J.D. Kelly, A.B. McEwen, P.J. Sadler, Contrast agent for NMR scanning, patent application no. 06/884,622, 1989.

[10] S.W.A. Bligh, C.T. Harding, A.B. McEwen, P.J. Sadler, J.D. Kelly, J.A. Marriott, Polyhedron, 13 (1994) 1937.

[11] M. Kueny-Stotz, A. Garofalo, D. Felder-Flesch, Eur. J. Inorg. Chem., (2012) 1987.

[12] H.B. Na, J.H. Lee, K. An, Y.I. Park, M. Park, I.S. Lee, D.-H. Nam, S.T. Kim, S.-H. Kim, S.-W. Kim, K.-H. Lim, K.-S. Kim, S.-O. Kim, T. Hyeon, Angew. Chemie Int. Ed., 46 (2007) 5397.
[13] H.B. Na, J.H. Lee, K. An, Y.I. Park, M. Park, I.S. Lee, D.-H. Nam, S.T. Kim, S.-H. Kim, S.-W. Kim, K.-H. Lim, K.-S. Kim, S.-O. Kim, T. Hyeon, Angew. Chemie, 119 (2007) 5493.
[14] T. Kim, E. Momin, J. Choi, K. Yuan, H. Zaidi, J. Kim, M. Park, N. Lee, M.T. McMahon, A. Quinones-Hinojosa, J.W.M. Bulte, T. Hyeon, A.A. Gilad, J. Am. Chem. Soc., 133 (2011) 2955.
[15] J. Zhu, E.M. Gale, I. Atanasova, T.A. Rietz, P. Caravan, Chem. Eur. J., 20 (2014) 14507.
[16] Z.P. Xu, N.D. Kurniawan, P.F. Bartlett, G.Q. Lu, Chem. Eur. J., 13 (2007) 2824.
[17] S.Y. Kim, J.-M. Oh, J.S. Lee, T.-J. Kim, J.-H. Choy, J. Nanosci. Nanotechnol., 8 (2008) 5181.
[18] J.-M. Oh, T.T. Biswick, J.-H. Choy, J. Mater. Chem., 19 (2009) 2553.
[19] M, Jin, D. E. M. Spillane, C. F. G. C. Geraldes, G. R. Williams, S. W. A. Bligh, Dalton Trans, 44 (2015) 20728.
[20] A. Merbach, L. Helm, E. Toth, The chemistry of contrast agents in medical magnetic resonance imaging, John Wiley & Sons Ltd, Chichester, 2013.
[21] P. Caravan, J.C. Amedio, S.U. Dunham, M.T. Greenfield, N.J. Cloutier, S.A. McDermid, M. Spiller, S.G. Zech, R.J. Looby, A.M. Raitsimring, T.J. McMurry, R.B. Lauffer, Chem. Eur. J., 11 (2005) 5866.
[22] S. Aime, M. Botta, S. G. Crich, G. B. Giovenzana, R. Pagliarin, M. Piccinini, M. Sisti and E. Terreno, J. Biol. Inorg. Chem., 2 (1997) 470.
[23] M. Botta, Eur. J. Inorg. Chem., (2000) 399.
[24] P. Lebduskova, P. Hermann, L. Helm, E. Toth, J. Kotek, K. Binnemans, J. Rudovsky, I. Lukes and A. E. Merbach, Dalton Trans., (2007) 493.
[25] Z. Kotkova, G. A. Pereira, K. Djanashvili, J. Kotek, J. Rudovsky, P. Hermann, L. V. Elst, R. N. Muller, C. F. G. C. Geraldes, I. Lukes and J. A. Peters, Eur. J. Inorg. Chem., (2009) 119.
[26] J. Oakes and E. G. Smith, J. Chem. Soc., Faraday Trans., 79 (1983) 543.
[27] J. J. Stezowsk, R. Countrym and J. L. Hoard, Inorg. Chem., 12, (1973) 1749.
[28] S. H. Koenig, C. Baglin and R. D. Brown, Magn. Reson. Med.,1 (1984) 496.
[29] J. S. Troughton, M. T. Greenfield, J. M. Greenwood, S. Dumas, A. J. Wiethoff, J. F. Wang, M. Spiller, T. J. McMurry and P. Caravan, Inorg. Chem., 43 (2004) 6313.
[30] R.B. Lauffer, Chem. Rev., 87 (1987) 901.
[31] M.T.M. Zaki, E.N. Rizkalla, Talanta, 27 (1980) 709.
[32] R. J. Motekait, I. Murase and A. E. Martell, J. Inorg. Nucl. Chem., 33 (1971) 3353.
[33] K. Popov, H. Ronkkomaki and L. H. J. Lajunen, Pure Appl. Chem., 73 (2001) 1641.
[34] S. Laus, R. Ruloff, E. Toth and A. E. Merbach, Chem. Eur. J., 9 (2003) 3555.
[35] S. Aime, P. L. Anelli, M. Botta, M. Brocchetta, S. Canton, F. Fedeli, E. Gianolio and E. Terreno, J. Biol. Inorg. Chem., 7 (2002) 58.